NEURAL REGENERATION RESEARCH
www.nrronline.org

Research Article

Nerve growth factor-basic fibroblast growth factor poly-lactide co-glycolid sustained-release microspheres and the small gap sleeve bridging technique to repair peripheral nerve injury

Ming Li[1, 2, 3, #], Ting-Min Xu[1, 2, #], Dian-Ying Zhang[1, #], Xiao-Meng Zhang[1], Feng Rao[2, 3], Si-Zheng Zhan[1], Man Ma[1], Chen Xiong[1], Xiao-Feng Chen[1], Yan-Hua Wang[1, *, #]

https://doi.org/10.4103/1673-5374.344842

Date of submission: July 24, 2021

Date of decision: October 8, 2021

Date of acceptance: March 31, 2022

Date of web publication: June 6, 2022

From the Contents

Graphical Abstract

A new type of microsphere combined with the small gap sleeve bridging technique to repair peripheral nerve injury

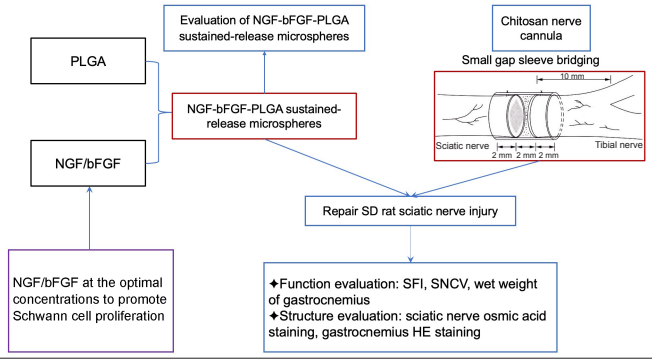

Abstract

We previously prepared nerve growth factor poly-lactide co-glycolid sustained-release microspheres to treat rat sciatic nerve injury using the small gap sleeve technique. Multiple growth factors play a synergistic role in promoting the repair of peripheral nerve injury; as a result, in this study, we added basic fibroblast growth factors to the microspheres to further promote nerve regeneration. First, in an *in vitro* biomimetic microenvironment, we developed and used a drug screening biomimetic microfluidic chip to screen the optimal combination of nerve growth factor/basic fibroblast growth factor to promote the regeneration of Schwann cells. We found that 22.56 ng/mL nerve growth factor combined with 4.29 ng/mL basic fibroblast growth factor exhibited optimal effects on the proliferation of primary rat Schwann cells. The successfully prepared nerve growth factor-basic fibroblast growth factor-poly-lactide-co-glycolid sustained-release microspheres were used to treat rat sciatic nerve transection injury using the small gap sleeve bridge technique. Compared with epithelium sutures and small gap sleeve bridging alone, the small gap sleeve bridging technique combined with drug-free sustained-release microspheres has a stronger effect on rat sciatic nerve transfection injury repair at the structural and functional level.

Key Words: biomimetic microfluidic chip; growth factor; *in vitro* biomimetic microenvironment; nerve function; peripheral nerve injury; sciatic nerve; small gap sleeve bridging; sustained-release microspheres

Introduction

Peripheral nerve injury is a common problem in trauma patients. There are nearly 20 million patients with peripheral nerve injury in China, and the number is increasing by approximately 1 million per year (Zhang et al., 2015a). Sensory and motor dysfunction in the dominating area after peripheral nerve injury seriously affects patient quality of life and imposes a heavy burden on families and society. The treatment of peripheral nerve injury has become a major health problem that must be solved (Wang et al., 2015; Chandran et al., 2016; Ma et al., 2016; Jiang et al., 2017; Ko et al., 2018; Qian et al., 2018; Qu et al., 2021).

At present, peripheral nerve injury repair methods include epineurial neurorrhaphy and autologous nerve transplantation. However, surgical epineurial neurorrhaphy cannot solve the large anastomotic tension and neurofibromatosis (Forbes and Rosenthal, 2014). Although autologous nerve transplantation solves the tension problem, it creates damage to the donor area and has low efficacy (Cheng and Chen, 2002), immune rejection, and infection (Ko et al., 2017). As a result, after the repair of peripheral nerve injury, autologous transplants are prone to slow nerve regeneration, twisted ends and scars, incomplete nerve regeneration, and muscle and target organ atrophy that seriously affect the structural and functional recovery of damaged nerves (Bikis et al., 2018; Ma et al., 2018).

Our previous studies found the following. 1) Based on the nerve cannula and surgery, the small gap sleeve bridging technique was proposed to replace the peripheral nerve epineurial neurorrhaphy technique that has been used for centuries. The small gap sleeve bridging technique has advantages of reducing neuroma, selective nerve regeneration, and convenient use (Jiang et al., 2010; Kou et al., 2013; Zhang et al., 2015b). 2) Nerve growth factor (NGF)-poly-lactide-co-glycolid (PLGA) sustained-release microspheres combined with the small gap sleeve bridging technique promoted the repair of rat sciatic nerve injury (Wang et al., 2014). The sustained-release microspheres combined with the small gap sleeve bridging technique provide an innovative solution to peripheral nerve injury; however, there are still urgent issues that need to be addressed, including the selection of the concentration of the sustain-released drugs, the effect of multiple sustained-release drugs (growth factors) used in combination, and how to improve their performance.

In this study, we used a drug-screening biomimetic microfluidic chip to

[1]Department of Trauma and Orthopedics, Peking University People's Hospital, Beijing, China; [2]Key Laboratory of Trauma and Neural Regeneration (Peking University), Ministry of Education, Beijing, China; [3]Trauma Medicine Center, Peking University People's Hospital; National Center for Trauma Medicine, Beijing, China

***Correspondence to:** Yan-Hua Wang, PhD, wangyanhua04119@pkuph.edu.cn.

https://orcid.org/0000-0003-1201-7216 (Yan-Hua Wang)

#These authors contributed equally to this work.

Funding: *This work was supported by the National Key Research and Development Program of China, No. 2016YFC1101603 (to DYZ); the National Natural Science Foundation of China, Nos. 31640045 (to YHW), 81901251 (to ML); the Natural Science Foundation of Beijing of China, No. 7204323 (to ML).*

How to cite this article: *Li M, Xu TM, Zhang DY, Zhang XM, Rao F, Zhan SZ, Ma M, Xiong C, Chen XF, Wang YH (2023) Nerve growth factor-basic fibroblast growth factor poly-lactide co-glycolid sustained-release microspheres and the small gap sleeve bridging technique to repair peripheral nerve injury. Neural Regen Res 18(1):162-169.*

simulate the body's microenvironment *in vitro* and then screened the optimal combination of NGF/basic fibroblast growth factor (bFGF) to promote Schwann cell regeneration in rats. Based on the selected drug gradients, we prepared PLGA sustained-release microspheres loaded with NGF and bFGF using a water/oil/water (W/O/W) double emulsion solvent evaporation method and evaluated their properties for optimization. We also used the prepared NGF-bFGF-PLGA sustained-release microspheres to repair rat sciatic nerve injury using the small gap sleeve (chitin nerve cannula) bridging technique and evaluated the efficacy at the structural and functional levels.

Methods

Construction of the drug screening biomimetic microfluidic chip

The drug screening biomimetic microfluidic chip mold was fabricated using Autodesk Computer Aided Design engineering drawing software (AutoCAD, Version 20.1, Autodesk Inc., San Rafael, CA, USA) and a soft lithography technique (Qin et al., 2010). The biomimetic microfluidic chip was prepared using polydimethylsiloxane and adhesive slides. The prepared drug screening biomimetic microfluidic chip device (Wenhao Co., Ltd., Suzhou, China) comprises a microflow pump, syringe, connecting catheters, joints, and microfluidic chips. The chip has a two-layer structure: the first layer is a polydimethylsiloxane material and the second layer is a glass base. The first layer of the chip has two liquid inlets, one liquid outlet, one drug concentration gradient generator, and eight sets of cell culture chambers. The liquid outlet and liquid inlet are connected by a plurality of microfluidic channels. The second layer of the chip is a glass base with the microflow pump, syringe, connecting conduits, joints, two inlet ports of the first layer pump through which the drug or growth factor is introduced into the chip, and the liquid outlet of the second layer of the chip that receives the waste liquid through the joints and the connecting catheters. After the drug is administered, the growth state of the cells in the cell culture chambers can be observed to investigate the drug efficacy.

Identification of the drug screening biomimetic microfluidic chip

In the biomimetic microfluidic chip, the drug-loaded liquid flows from Inlets 1 and 2, then goes through the CGG structure into the downstream parallel cell culture chamber under the action of an external flow pump, and the liquid finally flows out from the liquid outlet. With the help of CGG, Liquid 1 and Liquid 2 form different concentration gradients by constant mixing. According to the Reynolds effect (1883) and Jeon et al.'s previous work (Li Jeon et al., 2002; Sacchetti and Lambiase, 2017), when the liquid flows through the microchannel at a lower velocity, it will exist in the form of laminar flow. The fluid particle only follows the flow direction in a one-dimensional movement. There is no macroscopic mixing motion with the surrounding fluid. In the microfluidic device, the flow rate of the liquid was set to 0.1 μL/min, and different laminar fluids were designed to produce concentration gradients through curved microchannels (100 μm high, 200 μm wide). For example, when Inlet 1 is filled with a drug-free liquid and Inlet 2 is injected with the liquid containing drug R, the specific concentrations of the microfluidic device are 0, 1/7R, 2/7R, 3/7R, 4/7R, 5/7R, 6/7R, and 1R, respectively. In this study, to verify the performance of CGG, we injected phosphate-buffered saline (PBS) and acridine orange solution (AO, 5 μg/mL) into Inlets 1 and 2, respectively, and waited for a stable concentration gradient to form. The fluorescence intensity of each culture chamber was observed quantitatively using an inverted fluorescence microscope (Olympus, Shinjuku, Tokyo, Japan) and compared with theoretical values. All experimental results were repeated three times.

Isolation, culture, and identification of primary Schwann cells

This study was approved by the Ethics Review Board of Peking University People's Hospital (approval No. 2019PHE038) on November 11, 2019. The primary Schwann cells were cultured and obtained by double enzyme digestion. First, ten 24-hour-old specific pathogen-free Sprague-Dawley rats (Beijing Vital River Laboratory Animal Technology Co., Ltd., animal production license No. SCXK (Jing) 2016-0006, animal usage license No. SYXK (Jing) 2017-0022) were sacrificed by cervical dislocation after inhalational anesthesia with isoflurane (4% isoflurane in 100% medical oxygen, 2 L/min, RWD Life science Co., Ltd., Shenzhen, Guangdong Province, China) and immersed in 75% alcohol for 1 minute. The bilateral sciatic nerves were dissected under a dissecting microscope (OLYMPUS Co.). The attached soft tissues, blood vessels, and epithelium were removed and then transferred to a pre-cooled PBS solution for temporary storage. The sciatic nerve was cut into 1 mm^3 pieces with fiber scissors, digested with 0.25% trypsin (MilliporeSigma, Burlington, MA, USA) and 0.1% type I collagenase (MilliporeSigma) for 15 minutes, then neutralized with an equal volume of Dulbecco's modified Eagle medium complete medium (GIBCO BRL Co., Grand Island, NY, USA) and centrifuged (67.2 × *g*, 5 minutes). After removal of the supernatant, cells were collected, inoculated in a Petri dish, and then cultured in a cell culture incubator (Thermo Fisher Scientific Co., Waltham, MA, USA) at 37°C and 95% humidity. The cells were regularly observed under an inverted microscope (Olympus Co.). The cells passaged when they reached 85% confluency. The fast-growing fibroblasts were removed by the differential adhesion method (30 minutes) (Kreider et al., 1981) to improve the purity of the Schwann cell culture.

The S-100 immunofluorescence labeling method was used to identify Schwann cells. Schwann cells with a good growth state were selected, trypsin digested, neutralized, and centrifuged to prepare the cell suspension. Cells were inoculated into 6-well plates (adhesive coverslips) and cultured in a 37°C, 5% CO_2 incubator. The cells were periodically observed under an inverted microscope. When cells covered the climbing slides, they were rinsed with PBS (three times, 5 minutes), fixed with 4% paraformaldehyde for 15 minutes, followed by three 5 minute PBS washes. Subsequently, the cells were treated with 0.5% Triton-100 for 15 minutes, followed by three 5-minute PBS washes. After incubation with 10% goat serum (Hyclone, South Logan, UT, USA) for 30 minutes, the cells were rinsed again. Thereafter, anti-S100 antibody (primary antibody, 1:500, Cat# BM0120, RRID: AB_2716291, Boster Biological Technology Co., Wuhan, China) was added to cover the cell surface. Cells were incubated overnight at 4°C and rewarmed at 37°C for 1 hour the next day, followed by three 5 minute PBS washes. After the addition of fluorescein-conjugated AffiniPure goat anti-rabbit IgG (H + L) (secondary antibody, 1:250, Cat# ZF-0311, RRID: AB_2571576, Zhongshanjinqiao Biotec Co., Beijing, China), cells were incubated at 37°C for 30 minutes in the dark, followed by three 5-minute PBS washes. The cells were stained with Hoechst 33258 (0.5 μg/mL, MilliporeSigma), stored in the dark for 10 minutes, followed by three 5-minute PBS washes. Finally, the slides were stained with immunofluorescence dye, and cells were observed using a fluorescence microscope (Olympus).

Optimal combination of NGF/bFGF for Schwann cell proliferation based on a biomimetic microfluidic chip screening

Primary rat Schwann cells in the logarithmic growth phase were selected, treated with 0.25% trypsin, and neutralized with the same amount of Dulbecco's modified Eagle medium complete medium. The supernatant was discarded by centrifugation at 67.2 × *g* in a high-speed centrifuge (Eppendorf Co., Hamburg, Germany) for 5 minutes. The centrifuged cells were suspended in the appropriate amount of complete medium. The cell number was adjusted to a concentration of 1 × 10^5/mL using a blood cell counting plate (Beckman Coulter, Miami, FL, USA). Rat tail collagen solution (0.24%, MilliporeSigma) and an appropriate amount of 0.1 M hydrogen sodium oxide were combined to create a three-dimensional gel cell system. The Schwann cell-rat tail collagen mixture was quickly injected into the parallel cell culture chamber downstream of the microfluidic chip. The number of cells in each culture chamber was uniform and evenly distributed. The microfluidic chip was placed in a 37°C, 5% CO_2 cell culture incubator for 30 minutes to solidify the colloid. The microflow pump and other ancillary devices were connected, and the NGF complete medium (40 ng/mL) and bFGF-containing medium (10 ng/mL) were pumped into Inlet 1 and Inlet 2 at a rate of 0.1 μL/min. The concentration of the drug generated by the microfluidic chip CGG was as follows (**Figure 1**). The cells were cultured continuously and the cell growth state was observed periodically. Seventy-two hours later, the culture medium was changed, and acridine orange (AO)/propidium iodide (PI) stain was introduced. Under the fluorescence microscope, different fields of view were selected to investigate the effect of the drug on the cells. The cell proliferation rate was calculated according to the formula: cell proliferation rate = (cell number after culture with NGF and bFGF/initially implanted cell number) × 100%. The above experiments were independently repeated three times. The number of cells in the suspension was calculated using the following formula: the number of cells contained in 1 mL suspension = (total number of cells in four grids/4) × 10^4.

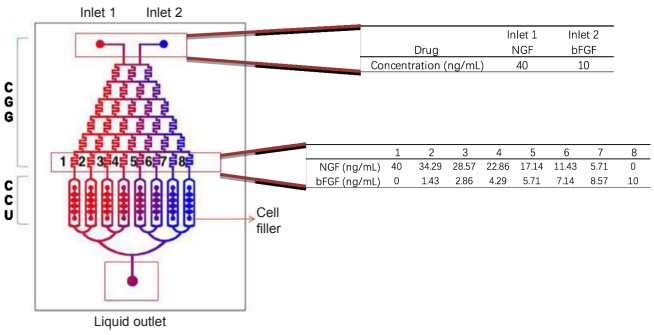

Figure 1 | **The schematic diagram of the drug screening biomimetic microfluidic chip.** bFGF: Basic fibroblast growth factor; CCU: cell culture unit; CGG: concentration gradient generator; NGF: nerve growth factor.

Preparation of the NGF-bFGF-PLGA sustained-release microspheres based on the drug concentrations obtained by chip screening

NGF-bFGF-PLGA sustained-release microspheres were prepared by the W/O/W double emulsion solvent evaporation method (Ashjari et al., 2012). PLGA sustained-release microspheres loaded with the most suitable combination of NGF and bFGF were prepared according to the following method. The optimum concentration of drug screening and drug encapsulation efficiency was 60%. First, specific amounts of NGF and bFGF, 10 mg bovine serum albumin, and 20 mg Tween-80 were added to 100 μM deionized water to prepare an internal aqueous phase (W1). Fifty milligrams of PLGA was dissolved in 2 mL of dichloromethane to prepare an oil phase (O). Thirty milliliters of 3% w/v polyvinyl alcohol solution was prepared as the external aqueous phase (W2). The inner aqueous phase W1 was then poured into the oil phase O and sonicated for 30 seconds to prepare colostrum (W1/O). After colostrum was poured into W2, the mixture was mechanically stirred at 100 × *g* for 5 minutes to prepare the double emulsion (W1/O/W2). The double emulsion was poured into 300 mL 0.1% (w/v) PVA. The residual organic solvent was volatilized for 3 hours using a magnetic stirrer at room temperature. The resulting microspheres were collected by centrifugation at 8000 × *g*. Finally, the microspheres were washed with deionized water

5 times, freeze-dried in a vacuum freeze dryer (Thermo Fisher Scientific, Waltham, MA, USA) for 48 hours, and stored at 4°C to produce NGF-bFGF-PLGA sustained-release microspheres. The amount of the loaded drug increased during the preparation of the high drug proportion drug-loaded microspheres. The same step was used to prepare the blank microspheres, except that drug was not loaded.

Evaluation of the NGF-bFGF-PLGA sustained-release microspheres

Morphological characterization

A small amount of sustained-release microspheres were dispersed in deionized water. The morphology of NGF-bFGF-PLGA sustained-release microspheres was observed under an inverted microscope and a scanning electron microscope (Hitachi, Tokyo, Japan). The average diameter and particle size distribution of the microspheres were analyzed with a laser particle size distribution analyzer (Beckman Coulter).

Sustained-release microsphere release curve

The standard curve of NGF was determined by high-performance liquid chromatography (Thermo Fisher Scientific). NGF was diluted with PBS to prepare 0, 1, 2, 3, 4, 5, and 10 μg/mL solutions. The mobile phase was acetonitrile/water (v/v) = 36/64. The flow rate was 1 mL/min. The absorbance at 280 nm was monitored with an ultraviolet optical detector (Eppendorf Co.). The standard curve was drawn according to the relationship between the absorbance at 280 nm and the different solution concentrations. All experiments were independently repeated three times.

Five milligrams of the NGF-bFGF-PLGA sustained-release microspheres (loading ratio 1000:1) were removed at room temperature, soaked in 2 mL PBS, and stored at 37°C. At different time points, 100 μL of the supernatant was removed after centrifugation to determine the NGF concentration using high-performance liquid chromatography. The remaining supernatant was discarded and the microspheres were resoaked in new 2 mL PBS and stored at 37°C. The amount of NGF released was calculated using the standard curve and the ratio obtained above. The release curve of the sustained release microsphere was estimated and prepared. All experiments were independently repeated three times.

Drug loading and encapsulation efficiency

Dried NGF-bFGF-PLGA sustained-release microspheres (loading ratio 1000:1) were dissolved in 500 μL of ethyl acetate. After the addition of 2 mL deionized water, the mixture was thoroughly mixed. After removal of the supernatant, NGF was extracted from ethyl acetate. The absorbance value of the supernatant at 280 nm was measured by high-performance liquid chromatography. The NGF level in the microspheres was evaluated according to the ratio obtained above. The drug-free microsphere degradation solution was used as a blank control, and all experiments were independently repeated three times. The drug loading and encapsulation efficiency were calculated using the following formulas: drug loading = drug content / microsphere mass; encapsulation efficiency = drug content / coagulant dosage.

Preparation of absorbable artificial biological nerve cannula

The absorbable artificial biological nerve cannula was prepared using chitosan (Fengrun Biotech, Taizhou, China) as the main raw material, and a hollow fiber spinning and drawing process was performed according to a previous study (Zhang et al., 2015b). Absorbable artificial biological nerve cannula combined with PLGA sustained-release microspheres loading different neurotrophic factors causes the bio-cannula to release drugs synchronously during the degradation process. The NGF-bFGF-PLGA sustained-release microspheres were established with a small gap sleeve bridging system to promote the repair of peripheral nerve damage.

Evaluation of NGF-bFGF-PLGA sustained-release microspheres combined with the small gap sleeve bridging technique for repairing sciatic nerve injury in rats and its therapeutic effect

Experimental animals

Twenty-four female Sprague-Dawley rats (6–8 weeks old, 200 g body weight, clear genetic background) were purchased from Beijing Vital River Laboratory Animal Technology Co., Ltd. The experimental animals were kept in a specific-pathogen-free cage of the Experimental Animal Center of Peking University People's Hospital, at room temperature 23 ± 2°C, and a relative humidity of 60–65%. The rats were allowed a free diet, fed standard pellet feed and clean drinking water, and maintained a daily 12-hour light/dark cycle.

Only female rats were used in this study because they have similar body weight and development as male rats at the same age and are less irritable. The experimental procedure and treatment followed the regulations of the Laboratory Animal Management Regulations of Peking University People's Hospital. All experiments were designed and reported according to the Animal Research: Reporting of *In Vivo* Experiments (ARRIVE) guidelines (Percie du Sert et al., 2020).

Establishment and repair of the rat sciatic nerve injury model

SD rats were anesthetized with isoflurane (RWD, San Diego, CA, USA) using a small animal anesthesia machine. The surgical area was sterilized with iodophor. A surgical incision was made on the posterior lateral side of the thigh. The sciatic nerve was fully exposed. An acute transverse injury model of the sciatic nerve was made by cutting the sciatic nerve 1 cm above the sciatic nerve bifurcation point (the phrenic nerve and common peroneal nerve) (Jiang et al., 2010; Zhang et al., 2015b). Rats were randomly divided into four groups: epithelium suture (n = 6); small gap sleeve bridging + saline (n = 6), small gap sleeve bridging + drug-free sustained-release microsphere (n = 6) and small gap sleeve bridging + NGF-bFGF-PLGA sustained-release microsphere (n = 6) groups. The microspheres (4 μL) were injected into the 2 mm gap of the conduit with a microinjector. The normal contralateral nerve of each group served as a negative control (n = 24). After suturing and sterilization of the wound, a small amount of picric acid was smeared on the wound to prevent the rats from biting each other (**Figure 2**). A conduit was placed between the two stumps while viewing under 4×. The 9-0 nylon suture penetrated the conduit wall from the external side to the inner side 1 mm from the conduit stump fringe. After suturing the epineurium, a suture needle was penetrated into the conduit wall from the inner side to the external side at the corresponding parallel site with the needling point. There was a 2-mm long gap between the two nerve stumps (considered a small gap). Nerve stumps were inserted approximately 1 mm into the conduit.

General observations

Twelve weeks after surgery, the general condition of the rats was observed, including the mobility of the surgical limbs, degree of wound healing, presence or absence of ulcers and infection, and presence or absence of toe ulcerations caused by autophagy.

Functional evaluation

Sciatic nerve function index: Twelve weeks after surgery, the sciatic functional index in each group was evaluated by a self-made footprint experiment transparent glass plate channel (100 cm long, 15 cm wide, 20 cm high) and a camera with video recording capabilities (Canon 60D, Canon, Tokyo, Japan). The experimental data of the surgical plantar was acquired via a post screenshot (**Figure 3**). The rats were placed on a transparent runway, and rat footprints were observed and captured through a 45° right angle mirror under the glass channel. Footprint parameters include the footprint length (PL, distance from heel to toe), toe spread (TS, distance from the first to the fifth toe), and intermediate toe distance (IT, distance from the second to the fifth toe). At the same time, the normal left toe parameters, NPL, NTS, and NIT, and the right (experimental) limb toe parameters EPL, ETS, EIT were recorded. The sciatic nerve function index was calculated according to the following formula (0 is normal, and –100 is complete damage): Sciatic nerve function index = –38.3 [(EPL – NPL)/NPL] + 109.5 [(ETS – NTS)/NTS] + 13.3 [(EIT – NIT)/NIT] – 8.8.

Nerve conduction velocity: Twelve weeks after surgery, the electrophysiological technique was used to evaluate the sciatic nerve conduction velocity of the limb. Rats were anesthetized with 2% sodium pentobarbital (30 mg/kg, intraperitoneally, Sinopharm Chemical Reagent Co., Ltd., Shanghai, China). Rat sciatic nerve was exposed. The stimulating electrodes (Xi'an Friendship Medical Electronics Co., Ltd., Xi'an, China) were placed at the proximal and distal ends of the mouse repair site. The recording electrode was inserted into the anterior tibial muscle and the ground electrode was placed on the ipsilateral thigh muscle. The nerve was stimulated with a rectangular pulse (duration 0.1 ms, 0.12 mA, 1 Hz) and the distance between the electrodes was accurately measured. The neural stimulation latency was recorded and the difference was calculated. The sciatic nerve conduction velocity was calculated semi-automatically according to the formula: sciatic nerve conduction velocity = conduction distance/latency difference. At the same time, the action potentials of the rats in each group were recorded, and the amplitudes were compared and evaluated (**Figure 4**).

Muscle wet weight: Twelve weeks after surgery, the rats were sacrificed by cervical dislocation after anesthesia with 2% sodium pentobarbital (30 mg/kg, intraperitoneally, Sinopharm Chemical Reagent Co., Ltd., Shanghai, China). The healthy and operated gastrocnemius of rats in each group were completely separated and immediately weighed (Shimadzu Co., Kyoto, Japan). The overall function of the muscles was evaluated by comparing the wet weight ratio of the experimental side and control side.

Pathological evaluation

Neurohistochemistry: Twelve weeks after surgery, bilateral sciatic nerves in each group were isolated for osmic acid staining. First, the sciatic nerve was fixed with 4% formaldehyde for 12 hours, rinsed with running water for 6 hours, stained with 1% osmic acid for 12 hours, and rinsed with running water for 6 hours. The sciatic nerve was then sequentially dehydrated with 50%, 70%, 75%, 80%, 85%, 90%, 95%, and 100% alcohol (two 15-minute washes for each solution), xylene transparent liquid once, and xylene transparent liquid for two 15 minute washes. The transparent nerve tissue was placed in a dipping wax for 90 minutes and then embedded on a cold bench. The tissue was cross sectioned with a microtome into 2–3 μm thick sections. The tissue sections were placed in an oven baking sheet (60°C, 1 hour), cooled to room temperature, and placed in a dewaxing liquid (three times, 5 minutes) to transparency. Finally, the tissue sections were sealed with a neutral resin and photographed under an upright microscope (Leica, Wetzlar, Germany). For counting axons after osmic acid staining, five fields (upper left, upper right, lower left, lower right, middle) were randomly selected using Image Pro Plus (Media Cybernetics, Inc., Rockville, MD, USA) to count the number and area of nerve fibers. The area of the nerve trunk (N1 = n/ds × s, n = counted number, ds = field area, s = total area) and quantity of the unit area of the myelinated nerve fibers were calculated, the nerve fibers not in the nerve trunk were manually counted as N2, the sum of the two is the total number of myelinated nerve fibers N = N1 + N2. All counts were independently repeated three times and averaged.

Muscle histology test: Twelve weeks after surgery, the fresh specimens of the gastrocnemius were removed and then immersed in a special small box with

an appropriate amount of optimal cutting temperature compound. The box was slowly placed in a small cup containing liquid nitrogen. When the bottom of the box contacted the liquid nitrogen, the sample began to freeze. Caution was made to avoid liquid nitrogen entering the small box. The tissue quickly froze into a solid after approximately 10–20 seconds. A layer of embedding glue was applied to the sample holder. The tissue was then placed on the sample holder and pre-cooled for 5–10 minutes to achieve the optimal cutting temperature compound to penetrate the tissue. The embedded tissue (muscle belly) was cut into 5-μm thick sections using the constant temperature ice slice (Leica). Tissue sections were then left at room temperature for 30 minutes, fixed in acetone at 4°C for 10 minutes, washed with PBS, stained with hematoxylin for 3 minutes (to the degree of over-staining), and washed with ethanol for 10 minutes. The tablets were reddish-brown, the tap water was anti-blue, and the nucleus was blue-purple. Subsequently, tissue sections were stained with eosin for 2 minutes, washed with water, dehydrated with alcohol gradients for 10 seconds, cleared with xylene I and xylene II, sealed with neutral resin, and observed with the fluorescence microscope.

Statistical analysis

No statistical methods were used to predetermine sample size; however, our sample sizes were similar to those reported in a previous publication (Zhang et al., 2015b). No animals or data points were excluded from the analysis. The evaluator was blinded to grouping. All data were statistically analyzed using SPSS 26.0 software (IBM Corp., Armonk, NY, USA) and expressed as the mean ± standard deviation (SD). One-way analysis of variance followed by the Bonferroni *post hoc* test was used for comparisons of groups. A level of $P < 0.05$ indicated statistical difference.

Results

Preparation of NGF-bFGF-PLGA sustained-release microspheres based on the microfluidic chip

Design of the drug screening biomimetic microfluidic chip

The microfluidic chip virtual model was designed using Autodesk AutoCAD software. The chip comprises an upstream CGG and downstream parallel cell culture unit (CCU). The chip was 45 mm long and 25 mm wide, including two inlet ports (1.4 mm in diameter), one liquid outlet (1.8 mm in diameter), one drug CGG, and eight cell culture chambers (1.2 mm × 700 μm × 100 μm). The liquid outlet was connected to the inlet ports by a plurality of microchannels (200 μm in width and 100 μm in height) (**Figure 5**). The chip base consisted of a clean, adhered glass backsheet.

Preparation of a drug screening biomimetic microfluidic chip

The chip mold was made by soft lithography, and the biomimetic microfluidic chip was prepared by polydimethylsiloxane and clean slides. After the preparation, the microflow pump, syringe, connecting conduit, joint, two liquid inlets, and one liquid outlet were connected to form the drug screening biomimetic microfluidic chip system.

Identification of the drug screening biomimetic microfluidic chip

To verify the performance of the microfluidic chip, CGG, PBS, and AO (5 μg/mL) were injected into Inlets 1 and 2, respectively. After a stable concentration gradient was formed, the individual cell culture chambers were viewed under an inverted fluorescence microscope to measure the fluorescence intensity, which was compared with theoretical values. The drug screening microfluidic chip system can form a stable concentration gradient, which met the needs of subsequent experiments (**Figure 6**).

Isolation, culture, and identification of primary Schwann cells

Schwann cells were successfully cultured by double enzyme digestion. The cells had a normal bipolar long spindle shape, the cells were slender, and the nucleus was oval or round. The immunohistochemical identification showed that the cell body of the Schwann cells was positive for S-100. The cultured primary Schwann cells had good purity and met the needs of subsequent experiments (**Figure 7**).

Optimal concentration combination screening of NGF/bFGF to promote the proliferation of Schwann cells

Schwann cells were seeded in a biomimetic microfluidic chip, and the NGF complete medium (40 ng/mL) and bFGF-containing complete medium (10 ng) were pumped at a constant rate from Inlets 1 and 2 at a rate of 0.1 (μL/min). After 72 hours, the 22.86 ng/mL NGF + 4.29 ng/mL bFGF group had the best proliferation effect. Therefore, such a growth factor concentration combination strategy was selected for subsequent experiments (**Figure 8**).

Preparation of the NGF-bFGF-PLGA sustained-release microspheres

According to the drug concentration obtained by the biomimetic microfluidic chip, NGF-bFGF-PLGA sustained-release microspheres were successfully prepared by the W/O/W double emulsion solvent evaporation method. The surface was smooth (**Figure 9**). The microspheres were spherical in appearance, with a normal distribution (**Figure 9**).

Evaluation and improvement of the NGF-bFGF-PLGA sustained-release microspheres

As shown in **Figure 10**, the particle size of the NGF-bFGF-PLGA sustained-release microspheres was 29.64 ± 14.03 μm. We concentrated on the sustained-release of NGF drugs and inferred the combined release rate of NGF and bFGF. The results of the *in vitro* drug release experiments showed that there was a drug burst release in the NGF-bFGF-PLGA sustained-release microspheres. The amount of drug released was approximately 40% of the total drug for the 1st week, and then gradually increased to approximately 60% in the 4th week. The release curve approached the platform and eventually ended with the degradation of PLGA. Additionally, the *in vitro* complete degradation experiments of the NGF-bFGF-PLGA drug-loaded microspheres showed that the drug encapsulation efficiency of the sustained-release microspheres was approximately 17.04%.

NGF-bFGF-PLGA sustained-release microspheres combined with the small gap sleeve bridging technique for repairing sciatic nerve injury in rats

Postoperative general observation

Twelve weeks after surgery, the rats in each group had excellent growth status; no autophagy occurred in the repaired limbs, all wounds healed well without ulceration, and there was no inflammatory reaction. As shown in **Figure 11**, after the incision, the epithelium suture group had neuroma formation at the nerve injury repair site, and there was more connective tissue hyperplasia around the nerve. There was no neuroma formation in the small gap sleeve bridging group, and the nerve cannula was not completely degraded. Neonatal axons grew into the center of the cannula and the connective tissue around the nerve was significantly less in the small gap sleeve bridging group than in the epithelium suture group. There was little differences in appearance among the small gap sleeve bridging + saline, small gap sleeve bridging + drug-free sustained-release microsphere, and small gap sleeve bridging + NGF-bFGF-PLGA sustained-release microsphere groups.

Functional evaluation

Twelve weeks after surgery, the sciatic nerve function index and wet weight of the gastrocnemius in the small gap sleeve bridging + saline, small gap sleeve bridging + drug-free sustained-release microsphere and small gap sleeve bridging + NGF-bFGF-PLGA sustained-release microsphere groups were larger than those in the epithelium suture group. The sciatic nerve function index and wet weight of the gastrocnemius were significantly greater in the small gap sleeve bridging + NGF-bFGF-PLGA sustained-release microsphere group than in other groups ($P < 0.05$; **Figures 12** and **13**).

Twelve weeks after surgery, the sciatic nerve conduction velocity (SNCV) in the small gap sleeve bridging + saline, small gap sleeve bridging + drug-free sustained-release microsphere, and small gap sleeve bridging + NGF-bFGF-PLGA sustained-release microsphere groups was significantly greater than those in the epithelium suture group and significantly less than those of the normal nerve. The medullary sciatic nerve conduction velocity was faster in the small gap sleeve bridging + NGF-bFGF-PLGA sustained-release microsphere group than in the other groups (all $P < 0.05$). According to the action potential waveform diagram, the amplitudes of the nerve waves were greater in the small gap sleeve bridging + saline, small gap sleeve bridging + drug-free sustained-release microsphere, and small gap sleeve bridging + NGF-bFGF-PLGA sustained-release microsphere groups than in the epithelium suture group. The amplitude of the nerve waves was less in the small gap sleeve bridging + NGF-bFGF-PLGA sustained-release microsphere group than in the normal control group; however, there was a significant difference compared with the other groups. These findings indicate that the myelinated sciatic nerve conduction function recovered better in the small gap sleeve bridging + NGF-bFGF-PLGA sustained-release microsphere group (**Figure 14**).

Structural evaluation

Twelve weeks after surgery, the distal nerve in each group was stained with osmic acid. The epithelium suture group had an irregular distribution of myelinated nerve fibers and more connective tissue, and the axons were different in size. Nerve regeneration was better in the small gap sleeve bridging group than in the epithelium suture group; however, it was still poorer than the normal nerve group. In the small gap sleeve bridging + NGF-bFGF-PLGA microsphere sustained-release group, the myelinated nerve fibers regenerated, and the nerve morphology was more regular, similar to normal nerves, and the connective tissue was less, which had better repair effect than the other groups (**Figure 15**).

The average diameter of the myelinated nerve fibers in each group was smaller than that of the normal sciatic nerve 12 weeks after surgery, and the thickness of the regenerated nerve fibers was not uniform. Necrotic marrow was occasionally observed. In the small gap sleeve bridging + saline, small gap sleeve bridging + drug-free sustained-release microsphere, and small gap sleeve bridging + NGF-bFGF-PLGA sustained-release microsphere groups, the nerve fiber diameter, axon area, and myelin thickness were greater than the epithelium suture group and were less than the normal group. The optimal repair effect was observed in the small gap sleeve bridging + NGF-bFGF-PLGA sustained-release microsphere group. The number of myelinated nerve fibers was greater in the small gap sleeve bridging + NGF-bFGF-PLGA sustained-release microsphere group than the other groups ($P < 0.05$; **Figure 16**).

Twelve weeks after surgery, the muscles (gastrocnemius) were stained by hematoxylin and eosin. Our results showed that muscle fibers in the epithelium suture group were severely atrophied, and there was a large amount of collagen fiber growth. In the small gap sleeve bridging + saline, small gap sleeve bridging + drug-free sustained-release microsphere, and small gap sleeve bridging + NGF-bFGF-PLGA sustained-release microsphere groups, atrophy was milder, the gastrocnemius fiber was fuller, and the cut surface was neater. These findings suggest that small gap sleeve bridging + saline, small gap sleeve bridging + drug-free sustained-release microsphere, and small gap sleeve bridging + NGF-bFGF-PLGA sustained-release microspheres promote the functional recovery of peripheral nerve innervated muscle. The optimal repair effect was observed in the small gap sleeve bridging + NGF-bFGF-PLGA sustained-release microsphere group (**Figure 17**).

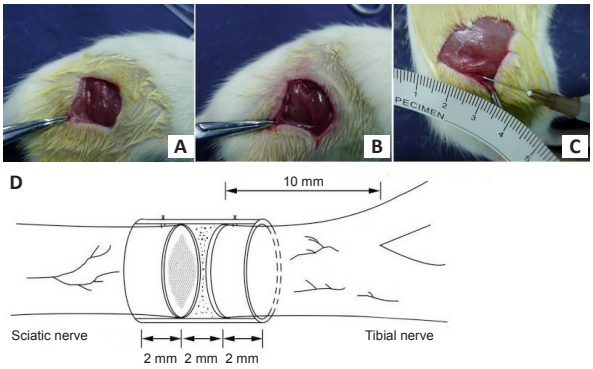

Figure 2 | Establishment and repair of a rat model of sciatic nerve injury.
(A) Sciatic nerve transverse injury. (B) Small gap sleeve bridging to repair sciatic nerve injury. (C) The NGF-bFGF-PLGA sustained-release microsphere combined with small gap sleeve bridging technique repairs sciatic nerve injury. Red arrows indicate sciatic nerve surgical sites. Blue arrow indicates small gap sleeve. (D) A schematic demonstrating the small gap sleeve bridging technique to repair sciatic nerve injury. NGF-bFGF-PLGA: Nerve growth factor basic-fibroblast growth factor poly-lactide co-glycolid.

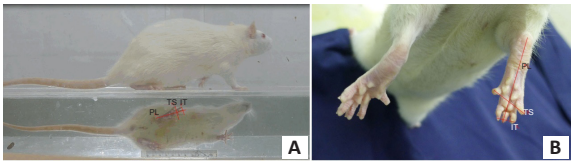

Figure 3 | Measurement of the parameters of the sciatic functional index.
(A) Walking trajectory of rats in a closed channel 12 weeks after surgery. (B) Foot length (PL), toe spread (TS), and intermediate toe distance (IT).

Figure 4 | Measurement of nerve conduction velocity and action potential in rats. The nerve was stimulated with a rectangular pulse (duration 0.1 ms, 0.12 mA, 1 Hz) and the distance between the electrodes was accurately measured. Sciatic nerve conduction velocity = conduction distance/latency difference.

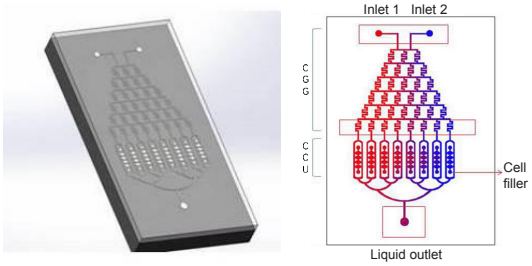

Figure 5 | Virtual model and schematic of a drug screening biomimetic microfluidic chip.
The chip comprises an upstream CGG and downstream parallel CCU, and includes two inlet ports, one liquid outlet, one drug CGG and eight cell culture chambers. CCU: Cell culture unit; CGG: concentration gradient generator.

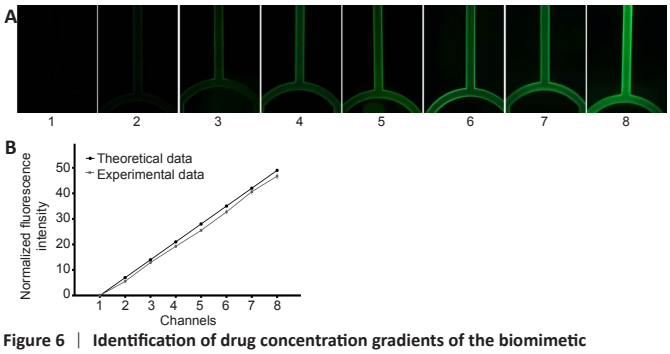

Figure 6 | Identification of drug concentration gradients of the biomimetic microfluidic chips.
(A) Images 1–8 represent eight concentration gradients (more details of concentrations are shown in Figure 1). (B) The difference between the theoretical and experimental data of a concentration gradient generator. Data are expressed as mean ± SD. The study was repeated three times.

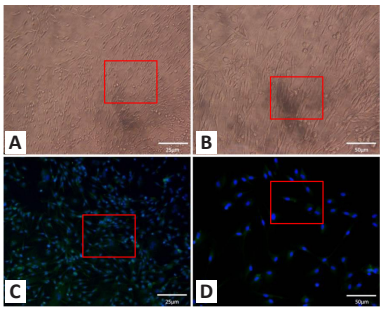

Figure 7 | Morphology and identification of primary Schwann cells.
(A, B) The morphology of primary Schwann cells viewed with an inverted microscope. Cells appeared to be bipolar long spindle shapes and the nucleus was oval or round. (C, D) Identification of primary Schwann cells under a fluorescence microscope. The cell bodies of Schwann cells were stained green (stained by fluorescein-isothiocyanate) by the S-100 protein antibody, and the nuclei were stained blue by Hoechst 33258. Scale bars: 25 μm in A, C; 50 μm in B, D. Red frames indicate the typical morphology of primary Schwann cells.

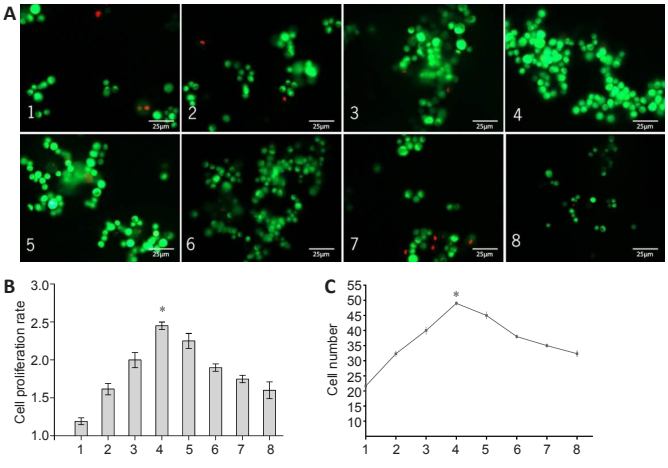

Figure 8 | Screening of the drug concentration in primary Schwann cells.
(A) Live and dead cell staining of rat Schwann cells under eight different NGF/bFGF drug concentrations on the microfluidic chip. Green is AO stained cells (live), red is PI stained cells (dead). The cell number and proliferation rate of Schwann cells gradually increased from the 1st chamber to the 4th chamber, and gradually decreased from the 4th chamber to the 8th chamber, reaching a peak in the 4th chamber (22.86 ng/mL NGF combined with 4.29 ng/mL bFGF). Scale bars: 25 μm. (B) Cell proliferation rate (cell number after culture with NGF/bFGF/initially implanted cell number × 100) under eight different concentrations. (C) Cell number after culture with NGF/bFGF under eight different drug concentrations. Data are expressed as mean ± SD. The above experiments were independently repeated three times. *$P < 0.05$, *vs.* other groups (one-way analysis of variance followed by Bonferroni *post hoc* test). 1–8: Cell culture chambers. AO: Acridine orange solution; bFGF: basic fibroblast growth factor; NGF: nerve growth factor; PI: propidium iodide.

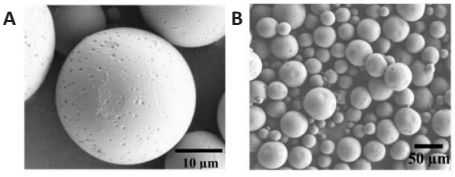

Figure 9 | Morphology of the sustained-release microspheres at different magnifications under the electron microscope.
Scale bars: 10 μm in A, 50 μm in B. NGF-bFGF-PLGA: Nerve growth factor basic fibroblast growth factor poly-lactide co-glycolid.

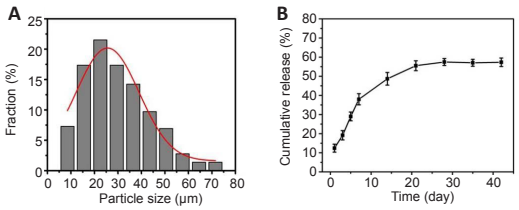

Figure 10 | Particle size (A) and drug release curve (B) of NGF-bFGF-PLGA sustained-release microspheres.
The red line indicates normal distribution. Data in B are expressed as mean ± SD. The experiments were independently repeated three times. NGF-bFGF-PLGA: Nerve growth factor basic fibroblast growth factor poly-lactide co-glycolid.

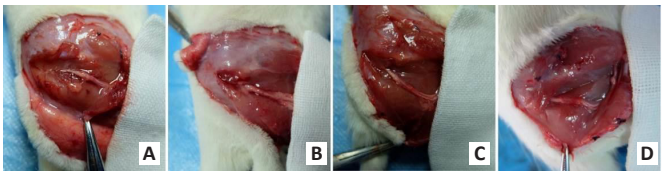

Figure 11 | Effect of NGF-bFGF-PLGA sustained-release microspheres on the general observation of the repair effect of sciatic nerve injury 12 weeks after surgery.
(A) Epithelium suture group. (B) Small gap sleeve bridging + saline group. (C) Small gap sleeve bridging + drug-free sustained release microsphere group. (D) Small gap sleeve bridging + NGF-bFGF-PLGA sustained-release microsphere administration group. The epithelium suture group had neuroma formation at the nerve injury repair site, and there is more connective tissue hyperplasia around the nerve than other groups. Neonatal axons grew into the center of the cannula and the connective tissue around the nerve was significantly less than the epithelium suture group. NGF-bFGF-PLGA: Nerve growth factor basic fibroblast growth factor poly-lactide co-glycolid.

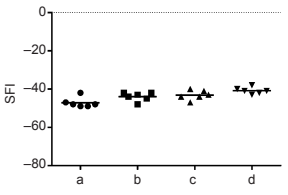

Figure 12 | Effect of NGF-bFGF-PLGA sustained-release microspheres on the sciatic functional index (SFI) of rats with sciatic nerve injury 12 weeks after surgery.
a–d: Epithelium suture group, small gap sleeve bridging + saline group, small gap sleeve bridging + drug-free sustained-release microsphere group, and small gap sleeve bridging + NGF-bFGF-PLGA sustained-release microsphere group. The sciatic nerve function index were significantly greater in the small gap sleeve bridging + NGF-bFGF-PLGA sustained-release microsphere group than in other groups.Data are expressed as mean (*n* = 6). NGF-bFGF-PLGA: Nerve growth factor basic fibroblast growth factor poly-lactide co-glycolid.

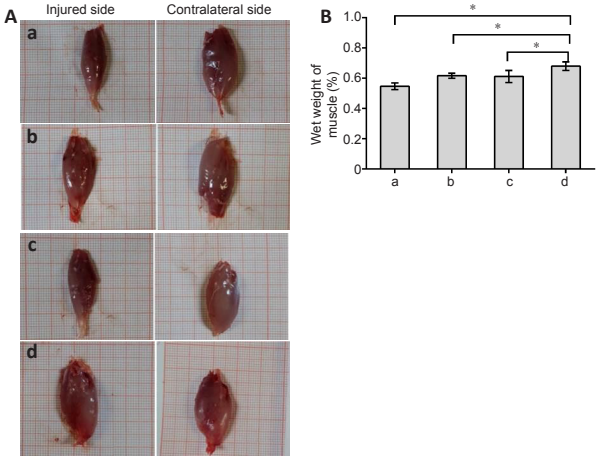

Figure 13 | Effect of NGF-bFGF-PLGA sustained-release microspheres on the wet weight of the gastrocnemius of rats with sciatic nerve injury 12 weeks after surgery.
(A) The appearance of the gastrocnemius in the injured and contralateral sides. (B) The wet weight ratio of gastrocnemius. a–d: Epithelium suture group, small gap sleeve bridging + saline group, small gap sleeve bridging + drug-free sustained-release microsphere group, and small gap sleeve bridging + NGF-bFGF-PLGA sustained-release microsphere group. Data are expressed as mean ± SD (*n* = 6). *$P < 0.05$ (one-way analysis of variance followed by Bonferroni *post hoc* test). NGF-bFGF-PLGA: Nerve growth factor basic fibroblast growth factor poly-lactide co-glycolid.

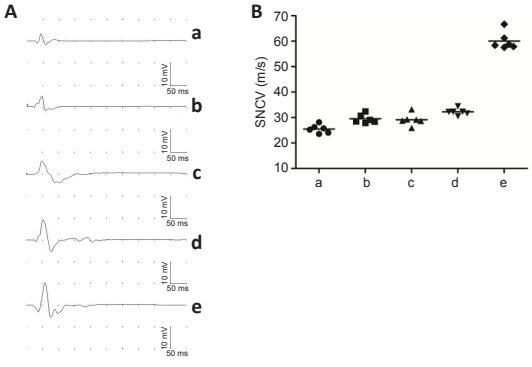

Figure 14 | Effect of NGF-bFGF-PLGA sustained-release microspheres on the SNCV and action potential of rats with sciatic nerve injury.
(A) Representative images of sciatic nerve electrophysiology. (B) Quantitative result of SNCV. Data are expressed as mean ± SD (*n* = 6). a–e: Epithelium suture group, small gap sleeve bridging + saline group, small gap sleeve bridging + drug-free sustained-release microsphere group, small gap sleeve bridging + NGF-bFGF-PLGA sustained-release microsphere group, and normal control side. NGF-bFGF-PLGA: Nerve growth factor basic fibroblast growth factor poly-lactide co-glycolid; SNCV: sciatic nerve conduction velocity.

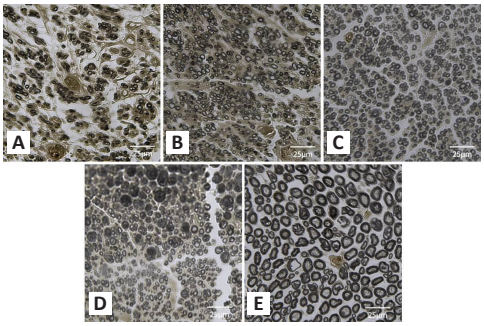

Figure 15 | Effects of NGF-bFGF-PLGA sustained-release microspheres on the myelinated nerve fibers in the sciatic nerve of rats with sciatic nerve injury (osmic acid staining).
(A) Epithelium suture group. (B) Small gap sleeve bridging + saline group. (C) Small gap sleeve bridging + drug-free sustained-release microsphere group. (D) Small gap sleeve bridging + NGF-bFGF-PLGA sustained-release microsphere group. (E) Normal contralateral sciatic nerve as a negative control. The nerve morphology in the small gap sleeve bridging + NGF-bFGF-PLGA sustained-release microsphere group was more regular and similar to normal nerves with less connective tissue, which had the best repair effect. Scale bars: 25 μm. NGF-bFGF-PLGA: Nerve growth factor basic fibroblast growth factor poly-lactide co-glycolid.

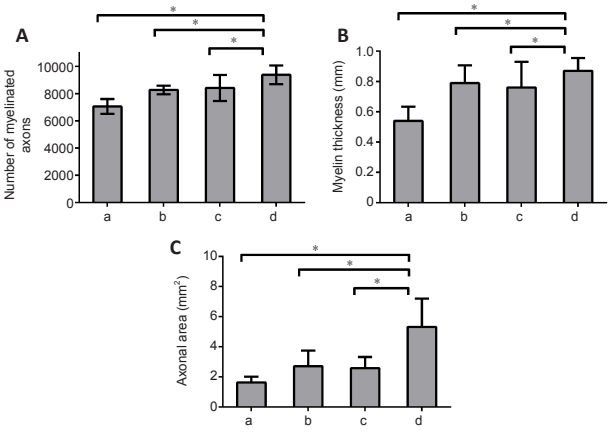

Figure 16 | Effects of NGF-bFGF-PLGA sustained-release microspheres on the number of nerve fibers (A), myelin thickness (B), and axonal area (C) of the distal sciatic nerve of rats with sciatic nerve injury.
Data are expressed as mean ± SD (*n* = 6). *$P < 0.05$ (one-way analysis of variance followed by Bonferroni *post hoc* test). a–d: Epithelium suture group, small gap sleeve bridging + saline group, small gap sleeve bridging + drug-free sustained-release microsphere group, and small gap sleeve bridging + NGF-bFGF-PLGA sustained-release microsphere group. NGF-bFGF-PLGA: Nerve growth factor basic fibroblast growth factor poly-lactide co-glycolid.

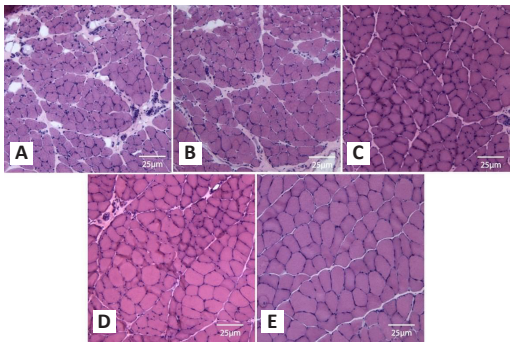

Figure 17 | Effects of NGF-bFGF-PLGA sustained-release microspheres on the gastrointestinal histological changes of rats with sciatic nerve injury (hematoxylin and eosin staining).
(A) Epithelium suture group. (B) Small gap sleeve bridging + saline group. (C) Small gap sleeve bridging + drug-free sustained-release microsphere group. (D) Small gap sleeve bridging + NGF-bFGF-PLGA sustained-release microsphere group. (E) Normal contralateral sciatic nerve as a negative control. Compared with the epithelium suture group, the gastrocnemius muscle fibers in the small gap sleeve bridging + saline, small gap sleeve bridging + drug-free sustained-release microsphere, and small gap sleeve bridging + NGF-bFGF-PLGA sustained-release microsphere groups were greater, and the those in the small gap sleeve bridging + NGF-bFGF-PLGA sustained-release microsphere group were even greater than in the other two groups. Scale bars: 25 μm. Red frames indicate typical histological performance in each image. NGF-bFGF-PLGA: Nerve growth factor basic fibroblast growth factor poly-lactide co-glycolid.

Discussion

Epineurial neurorrhaphy and autologous nerve transplantation are available for clinical treatment of peripheral nerve injury. However, epineurial neurorrhaphy has the drawback of fibroma proliferation and poor nerve regeneration. Autologous nerve transplantation has the disadvantages of limited source, donor site destruction, and the graft nerve is single (Jiang et al., 2010, 2017; Kehoe et al., 2012). Previous studies (Jiang et al., 2010; Kou et al., 2013; Zhang et al., 2015b) demonstrated that the small gap sleeve bridging technique based on a biodegradable bio-cannula for peripheral nerve anastomosis can reduce the operation time, reduce trauma, increase the accuracy of axon regeneration, reduce the formation of neurofibromatosis, and prevent the dominating muscle atrophy to improve the structural and functional repair effects after peripheral nerve injury. In this study, we used the small gap sleeve bridging technique combined with sustained-release microspheres loaded with multiple growth factors to further promote the therapeutic effect of peripheral nerve injury. This was the basic idea and starting point of this study.

The effect of growth factors on the repair of peripheral nerve injury has been recognized worldwide (Lien et al., 2020; Idrisova et al., 2022). Growth factor released locally after nerve injury will participate in the regeneration, migration, proliferation, differentiation, and regulation of various nerve cells (Gong et al., 2022; Idrisova et al., 2022). In the distal injured nerve, Schwann cells deprived of axonal contact proliferate, upregulate the synthesis and release of a variety of neurotrophic factors and basal lamina components that create an appropriate microenvironment for regenerating axons (Liu et al., 2014). Accumulating evidence indicates that following injury, regenerating axons are unable to cross a peripheral nerve gap without Schwann cell guidance at their migrating growth front (Cattin et al., 2015; Dun and Parkinson, 2015; Chen et al., 2019). Napoli et al. (2012) indicated that Schwann cells dedifferentiate to a progenitor-like state and proliferate, forming bands of Büngner upon which axons can regrow with a growth factor after peripheral nerve injury. Studies have demonstrated that multiple growth factors can play a synergistic role in promoting the repair of peripheral nerve injury (Frostick et al., 1998; Önger et al., 2017; Sacchetti and Lambiase, 2017). After nerve injury, the supply of neurotrophic factors in the distal axon was interrupted, the neuronal cell body degenerated, and the content of proximal axon neurotrophic factor decreased sharply, while the neurotrophin receptor increased rapidly (Keefe et al., 2017). Therefore, the local administration of a variety of exogenous NGFs in the damaged nerve will satisfy the need for nerve regeneration, and promote the structural regeneration and functional recovery of peripheral nerves. Currently identified growth factors that promote nerve regeneration include nerve growth factor, basic fibroblast growth factor, ciliary neurotrophic factor, glial cell line-derived neurotrophic factor, and brain-derived neurotrophic factor (Li et al., 2017). In this study, we selected two growth factors, NGF and bFGF, as loaded drugs. The combined application of growth factors promoted the regeneration and repair of peripheral nerve injury, which may be related to the following mechanisms. NGF and bFGF have a clear role in the initial stage of nerve injury repair, and NGF mainly manifests in stimulating neuronal synaptic growth, guiding axon directional growth, promoting neuronal differentiation, and neurotrophic chemotaxis. bFGF mainly promotes neuromyelination, accelerates Schwann cell proliferation, inhibits Schwann cell apoptosis, and improves angiogenesis and microcirculation. A previous study has shown the synergistic effects of the two factors (Wang et al., 2014).

The traditional intravenous administration method causes the growth factor to be eliminated by the reticuloendothelial system in a short time period (Tria et al., 1994). Therefore, the growth factor can only play a role in promoting nerve regeneration in a short time period (within 1 week), and the therapeutic effect is not satisfactory. Previous studies have found that the slow release of NGF-PLGA drug-loaded sustained-release microspheres prepared by the W/O/W double emulsion solvent evaporation method can increase the number of regenerated nerve fibers, promote the maturation of nerve fibers, and improve the function of the sciatic nerve (Péan et al., 1998; Sun et al., 2014). This method provides a possible solution to address the short-term inactivation of growth factors and greatly promotes the regeneration and repair of peripheral nerve injury. In this study, we continued to improve the above methods to achieve the effect of promoting peripheral nerve injury and regeneration by preparing sustained-release microspheres loaded with various growth factors such as NGF and bFGF. In the preparation of sustained-release microspheres, we chose PLGA as a drug carrier material. PLGA has good biocompatibility, mild and controllable degradability, and low immunity. PLGA is often used as a drug (drug, protein, peptide) matrix of sustained-release microspheres, which is widely used in the field of biomedicine (Ghorbani et al., 2017; Liu et al., 2017). Since PLGA is randomly polymerized from two monomers, lactic acid and glycolic acid, it is hydrolyzed and then metabolized to CO_2 and water, which is not harmful to humans (Semete et al., 2010). Because of the excellent biocompatibility and safety, PLGA has been certified by the US Food and Drug Administration. Therefore, this study did not specifically verify the biocompatibility and safety of the sustained-release microspheres.

How to find the optimal combination and concentration of NGF and bFGF to promote peripheral nerve regeneration and repair is an issue. Traditional drug screening methods are mainly based on the 3-(4,5-dimethyl-2-thiazolyl)-2,5-diphenyl-2H-tetrazolium bromide assay and cell counting kit-8 assay; however, these methods are different from the three dimensional, fluid, and complex internal environment in the human body because of their two-dimensional and static culture media, which greatly reduces their clinical practical value. As a result, the development of new drug screening methods is crucial. In this study, we used our designed drug screening biomimetic microfluidic chip to screen the optimal combination and concentration of NGF and bFGF for promoting peripheral nerve regeneration and repair. The microfluidic chip is a fast and efficient drug screening device. As a result, we successfully obtained the results of eight different drug concentration combinations of NGF and bFGF to promote Schwann cell regeneration. Our study revealed that NGF at 22.86 ng/mL + bFGF at 4.29 ng/mL had the best effect on peripheral nerve regeneration. Although the combined concentration of NGF and bFGF was less than the concentration of the single action, it had a better effect and may be related to its synergistic effect. Based on the drug screening results, we prepared NGF-bFGF-PLGA sustained-release microspheres and continued to improve them according to their drug loading and encapsulation efficiency. Our results showed that the self-designed drug screening biomimetic microfluidic chip can continuously supply fresh nutrients and oxygen to the three-dimensional cultured Schwann cells in a controlled fluid medium, and the chip can efficiently screen out the combined concentration of NGF and bFGF, promoting peripheral nerve regeneration.

Our study improved the technique of drug-loaded sustained-release microspheres and the highlights are as follows. 1) The technique promoted a single-factor drug sustained-release microsphere to a multi-factor drug-loaded sustained-release microsphere, which made it easier to improve the microenvironment of peripheral nerve injury, improving the growth rate and accuracy of the axons. 2) The drug screening biomimetic microfluidic chip was designed to simulate the three-dimensional dynamic growth state of Schwann cells *in vitro*, which provides a new way to select the drug loading of sustained-release microspheres. 3) The preparation of sustained-release microspheres was improved. By referring to the pre-study drug encapsulation rate and drug release rate, the drug loading during the preparation of the sustained-release microspheres was improved, and the sustained-release amount of the drug-loaded microspheres is closer to the normal physiological requirement for a better therapeutic effect. 4) Finally, high-performance liquid chromatography was used for measuring the characteristics and drug release of the microspheres, which greatly reduced the cost of testing and may inspire other drug loading research.

In the animal experiment of this study, we compared the repairing effect of peripheral nerve injury in rats of NGF-bFGF-PLGA sustained-release microspheres with small gap sleeve bridging, drug-free PLGA microsphere small gap sleeve bridging, simple small gap sleeve bridging, and epineurial neurorrhaphy. After 12 weeks, NGF-bFGF-PLGA microsphere sustained-release with the small gap sleeve bridging group exhibited better performance at the structural level (sciatic nerve osmic staining, nerve fiber count, myelin thickness, axon area, gastrocnemius hematoxylin and eosin staining) and functional level (sciatic nerve function index, muscle wet weight, nerve conduction velocity, action potential amplitude) than other experimental groups.

There are also shortcomings of this study. For example, considering the complex internal environment changes and the lack of *in vivo* observation methods, we could not achieve a one-to-one correspondence between the concentration of sustained-release drug *in vitro* and the concentration of sustained-release drug *in vivo*, which limits the value of the drug screening biomimetic microfluidic chip. The microfluidic chip we are currently using is relatively simple. Future research will include screening the drug concentration in a three-dimensional flow environment to simulate human organs. Although the application of NGF-bFGF-PLGA sustained-release microspheres with the small gap sleeve bridging to repair peripheral nerve injury in rats had positive results, primate models will have greater clinical value and significance. Overall, this study is an innovative test of repair methods after peripheral nerve injury; however, it lacks the molecular biological mechanism, and we will conduct more molecular biological research.

The optimal combination of NGF/bFGF to promote the proliferation of primary Schwann cells in rats was obtained by a drug screening biomimetic microfluidic chip. The NGF-bFGF-PLGA composite drug-loaded sustained-release microspheres were prepared based on the drug screening results. Animal experiments were used to confirm that the NGF-bFGF-PLGA composite drug-loaded sustained-release microsphere combined with the small gap sleeve bridging technique can promote the regeneration and repair of peripheral nerve injury.

In summary, we successfully carried out the concentration screening of multiple growth factors using our developed drug screening biomimetic microfluidic chip. We combined the sustained-release microsphere technology with the small gap sleeve bridging technique to repair sciatic nerve injury in SD rats. Findings from this study will help us apply the biomimetic microfluidic chip precise drug screening + drug-loaded degradable material sustained-release microspheres + small gap sleeve bridging technique to treat peripheral nerve injury. Findings from this study can be used as a reference for developing novel treatments of peripheral nerve injury.

Author contributions: *All authors contributed to study conception, manuscript writing and revision, critical review, and approved the final version of this manuscript.*
Conflicts of interest: *None declared.*

References

Ashjari M, Khoee S, Mahdavian AR (2012) Controlling the morphology and surface property of magnetic/cisplatin-loaded nanocapsules via W/O/W double emulsion method. Colloids Surf Physicochem Eng Aspects 408:87-96.

Bikis C, Degrugillier L, Thalmann P, Schulz G, Müller B, Hieber SE, Kalbermatten DF, Madduri S (2018) Three-dimensional imaging and analysis of entire peripheral nerves after repair and reconstruction. J Neurosci Methods 295:37-44.

Cattin AL, Burden JJ, Van Emmenis L, Mackenzie FE, Hoving JJ, Garcia Calavia N, Guo Y, McLaughlin M, Rosenberg LH, Quereda V, Jamecna D, Napoli I, Parrinello S, Enver T, Ruhrberg C, Lloyd AC (2015) Macrophage-Induced Blood Vessels Guide Schwann Cell-Mediated Regeneration of Peripheral Nerves. Cell 162:1127-1139.

Chandran V, Coppola G, Nawabi H, Omura T, Versano R, Huebner EA, Zhang A, Costigan M, Yekkirala A, Barrett L, Blesch A, Michaelevski I, Davis-Turak J, Gao F, Langfelder P, Horvath S, He Z, Benowitz L, Fainzilber M, Tuszynski M, et al. (2016) A systems-level analysis of the peripheral nerve intrinsic axonal growth program. Neuron 89:956-970.

Chen B, Chen Q, Parkinson DB, Dun XP (2019) Analysis of Schwann cell migration and axon regeneration following nerve injury in the sciatic nerve bridge. Front Mol Neurosci 12:308.

Cheng B, Chen Z (2002) Fabricating autologous tissue to engineer artificial nerve. Microsurgery 22:133-137.

Dun XP, Parkinson DB (2015) Visualizing peripheral nerve regeneration by whole mount staining. PLoS One 10:e0119168.

Forbes SJ, Rosenthal N (2014) Preparing the ground for tissue regeneration: from mechanism to therapy. Nat Med 20:857-869.

Frostick SP, Yin Q, Kemp GJ (1998) Schwann cells, neurotrophic factors, and peripheral nerve regeneration. Microsurgery 18:397-405.

Ghorbani F, Zamanian A, Nojehdehian H (2017) Effects of pore orientation on in-vitro properties of retinoic acid-loaded PLGA/gelatin scaffolds for artificial peripheral nerve application. Mater Sci Eng C Mater Biol Appl 77:159-172.

Gong C, Zhang YQ, Wang W (2022) Role and mechanism of cell therapy in repair of peripheral nerve injury. Zhongguo Zuzhi Gongcheng Yanjiu 26:2114-2119.

Idrisova KF, Zeinalova AK, Masgutova GA, Bogov AA, Allegrucci C, Syromiatnikova VY, Salafutdinov, II, Garanina EE, Andreeva DI, Kadyrov AA, Rizvanov AA, Masgutov RF (2022) Application of neurotrophic and proangiogenic factors as therapy after peripheral nervous system injury. Neural Regen Res 17:1240-1247.

Jiang B, Zhang P, Jiang B (2010) Advances in small gap sleeve bridging peripheral nerve injury. Artif Cells Blood Substit Immobil Biotechnol 38:1-4.

Jiang BG, Han N, Rao F, Wang YL, Kou YH, Zhang PX (2017) Advance of peripheral nerve injury repair and reconstruction. Chin Med J (Engl) 130:2996-2998.

Keefe KM, Sheikh IS, Smith GM (2017) Targeting neurotrophins to specific populations of neurons: NGF, BDNF, and NT-3 and their relevance for treatment of spinal cord injury. Int J Mol Sci 18:548.

Kehoe S, Zhang XF, Boyd D (2012) FDA approved guidance conduits and wraps for peripheral nerve injury: a review of materials and efficacy. Injury 43:553-572.

Ko CH, Shie MY, Lin JH, Chen YW, Yao CH, Chen YS (2017) Biodegradable bisvinyl sulfonemethyl-crosslinked gelatin conduit promotes regeneration after peripheral nerve injury in adult rats. Sci Rep 7:17489.

Ko HG, Choi JH, Park DI, Kang SJ, Lim CS, Sim SE, Shim J, Kim JI, Kim S, Choi TH, Ye S, Lee J, Park P, Kim S, Do J, Park J, Islam MA, Kim HJ, Turck CW, Collingridge GL, et al. (2018) Rapid turnover of cortical NCAM1 regulates synaptic reorganization after peripheral nerve injury. Cell Rep 22:748-759.

Kou Y, Peng J, Wu Z, Yin X, Zhang P, Zhang Y, Weng X, Qiu G, Jiang B (2013) Small gap sleeve bridging can improve the accuracy of peripheral nerve selective regeneration. Artif Cells Nanomed Biotechnol 41:402-407.

Kreider BQ, Messing A, Doan H, Kim SU, Lisak RP, Pleasure DE (1981) Enrichment of Schwann cell cultures from neonatal rat sciatic nerve by differential adhesion. Brain Res 207:433-444.

Li Jeon N, Baskaran H, Dertinger SK, Whitesides GM, Van de Water L, Toner M (2002) Neutrophil chemotaxis in linear and complex gradients of interleukin-8 formed in a microfabricated device. Nat Biotechnol 20:826-830.

Li R, Ma J, Wu Y, Nangle M, Zou S, Li Y, Yin J, Zhao Y, Xu H, Zhang H, Li X, Ye QS, Wang J, Xiao J (2017) Dual delivery of NGF and bFGF coacervater ameliorates diabetic peripheral neuropathy via inhibiting Schwann cells apoptosis. Int J Biol Sci 13:640-651.

Lien BV, Brown NJ, Ransom SC, Lehrich BM, Shahrestani S, Tafreshi AR, Ransom RC, Sahyouni R (2020) Enhancing peripheral nerve regeneration with neurotrophic factors and bioengineered scaffolds: A basic science and clinical perspective. J Peripher Nerv Syst 25:320-334.

Liu F, Zhang H, Zhang K, Wang X, Li S, Yin Y (2014) Rapamycin promotes Schwann cell migration and nerve growth factor secretion. Neural Regen Res 9:602-609.

Liu H, Lv P, Zhu Y, Wu H, Zhang K, Xu F, Zheng L, Zhao J (2017) Salidroside promotes peripheral nerve regeneration based on tissue engineering strategy using Schwann cells and PLGA: in vitro and in vivo. Sci Rep 7:39869.

Ma B, Liu X, Huang X, Ji Y, Jin T, Ma K (2018) Translocator protein agonist Ro5-4864 alleviates neuropathic pain and promotes remyelination in the sciatic nerve. Mol Pain 14:1744806917748019.

Ma J, Yu H, Liu J, Chen Y, Wang Q, Xiang L (2016) Curcumin promotes nerve regeneration and functional recovery after sciatic nerve crush injury in diabetic rats. Neurosci Lett 610:139-143.

Napoli I, Noon LA, Ribeiro S, Kerai AP, Parrinello S, Rosenberg LH, Collins MJ, Harrisingh MC, White IJ, Woodhoo A, Lloyd AC (2012) A central role for the ERK-signaling pathway in controlling Schwann cell plasticity and peripheral nerve regeneration in vivo. Neuron 73:729-742.

Önger ME, Delibaş B, Türkmen AP, Erener E, Altunkaynak BZ, Kaplan S (2017) The role of growth factors in nerve regeneration. Drug Discov Ther 10:285-291.

Péan JM, Venier-Julienne MC, Boury F, Menei P, Denizot B, Benoit JP (1998) NGF release from poly(D,L-lactide-co-glycolide) microspheres. Effect of some formulation parameters on encapsulated NGF stability. J Control Release 56:175-187.

Percie du Sert N, Hurst V, Ahluwalia A, Alam S, Avey MT, Baker M, Browne WJ, Clark A, Cuthill IC, Dirnagl U, Emerson M, Garner P, Holgate ST, Howells DW, Karp NA, Lazic SE, Lidster K, MacCallum CJ, Macleod M, Pearl EJ, et al. (2020) The ARRIVE guidelines 2.0: Updated guidelines for reporting animal research. PLoS Biol 18:e3000410.

Qian Y, Zhao X, Han Q, Chen W, Li H, Yuan W (2018) An integrated multi-layer 3D-fabrication of PDA/RGD coated graphene loaded PCL nanoscaffold for peripheral nerve restoration. Nat Commun 9:323.

Qin D, Xia Y, Whitesides GM (2010) Soft lithography for micro- and nanoscale patterning. Nat Protoc 5:491-502.

Qu WR, Zhu Z, Liu J, Song DB, Tian H, Chen BP, Li R, Deng LX (2021) Interaction between Schwann cells and other cells during repair of peripheral nerve injury. Neural Regen Res 16:93-98.

Sacchetti M, Lambiase A (2017) Neurotrophic factors and corneal nerve regeneration. Neural Regen Res 12:1220-1224.

Semete B, Booysen L, Lemmer Y, Kalombo L, Katata L, Verschoor J, Swai HS (2010) In vivo evaluation of the biodistribution and safety of PLGA nanoparticles as drug delivery systems. Nanomedicine 6:662-671.

Sun H, Xu F, Guo D, Liu G (2014) In vitro evaluation of the effects of various additives and polymers on nerve growth factor microspheres. Drug Dev Ind Pharm 40:452-457.

Tria MA, Fusco M, Vantini G, Mariot R (1994) Pharmacokinetics of nerve growth factor (NGF) following different routes of administration to adult rats. Exp Neurol 127:178-183.

Wang EW, Zhang J, Huang JH (2015) Repairing peripheral nerve injury using tissue engineering techniques. Neural Regen Res 10:1393-1394.

Wang Z, Han N, Wang J, Zheng H, Peng J, Kou Y, Xu C, An S, Yin X, Zhang P, Jiang B (2014) Improved peripheral nerve regeneration with sustained release nerve growth factor microspheres in small gap tubulization. Am J Transl Res 6:413-421.

Zhang PX, Yin XF, Kou YH, Xue F, Han N, Jiang BG (2015a) Neural regeneration after peripheral nerve injury repair is a system remodelling process of interaction between nerves and terminal effector. Neural Regen Res 10:52.

Zhang PX, A LY, Kou YH, Yin XF, Xue F, Han N, Wang TB, Jiang BG (2015b) Biological conduit small gap sleeve bridging method for peripheral nerve injury: regeneration law of nerve fibers in the conduit. Neural Regen Res 10:71-78.

C-Editor: Zhao M; S-Editors: Yu J, Li CH; L-Editors: Cooper A, Song LP; T-Editor: Jia Y